UNLV | UNIVERSITY LIBRARIES

8-2011

New cross sections for H on H2 collisional transitions

Qianxia Zou
University of Nevada, Las Vegas

Repository Citation

NEW CROSS SECTIONS FOR H ON H$_2$ COLLISIONAL TRANSITIONS

By

Qianxia Zou

Bachelor of Science (Physics)
Southeast University, China
2009

A thesis submitted in partial fulfillment
of the requirements for the

Master of Science in Physics
Department of Physics and Astronomy
College of Science

Graduate College
University of Nevada, Las Vegas
August 2011

We recommend the thesis prepared under our supervision by

Qianxia Zou

entitled

New Cross Sections for H on H$_2$ Collisional Transitions

be accepted in partial fulfillment of the requirements for the degree of

Master of Science in Physics

Department of Physics and Astronomy

Stephen Lepp, Committee Chair

Bing Zhang, Committee Member

Tao Pang, Committee Member

Balakrishnan Naduvalath, Graduate College Representative

Ronald Smith, Ph. D., Vice President for Research and Graduate Studies
and Dean of the Graduate College

August 2011

ABSTRACT

New Cross Sections for H on H$_2$
Collisional Transitions

by

Qianxia Zou

Dr. Stephen Lepp, Examination Committee Chair
Professor of Physics
University of Nevada, Las Vegas

The cross section for H on H$_2$ collisions is important for astrophysics as well as

our understanding of the simple chemical systems. This is the simplest atom-molecule

cross section. With a new H$_3$ potential surface by Mielke et al., we have modified the

ABC code by Skouteris, Castillo and Manolopoulos to calculate new cross sections.

These cross sections are compared to previous cross section calculations.

TABLE OF CONTENTS

LIST OF FIGURES

CHAPTER 1

INTRODUCTION

This thesis contains a study the quantum mechanical calculation of the H on H_2 cross section calculated with the ABC code. The ABC code uses a close-coupled approximation to do a quantum calculation on a potential surface and produce a state to state S-matrix[1]. For this thesis we have used the Mielke's potential surface[2], this builds on the work of David Archer[3] who did a similar calculation with the BKMP potential[4]. The new calculation is compared to that of Archer as well as others.

CHAPTER 2

APPLICATION IN ASTROPHYSICS

Since its discovery in 1671 by Robert Boyle, hydrogen has been an important element. It is the simplest atom. The energy level of hydrogen is one of the few problems which can be solved analytically[5]. Studying hydrogen has significant meaning to astrophysics.

Hydrogen is the lightest and most abundant chemical element, constituting roughly 75% of the universe's chemical elemental mass and over 90% by number of atoms. This element is found in great number in stars and gas giant planets. Molecular clouds of H_2 are associated with star formation. Also hydrogen is the most important reactant in the powering stars through proton-proton reaction and CNO cycle nuclear fusion. Throughout the universe, most of the hydrogen is in the atomic and plasma states. Stars in the main sequence are mainly composed of hydrogen in its plasma state.

Hydrogen is both an important cooling mechanism and diagnostic for astrophysics. As the massive element, most of the cooling of the first objects occurs through molecular hydrogen. To calculate this cooling requires collisional cross sections and Einstain A-values. These reactions are crucial to the thermal balance of the medium. Rovibrationally inelastic scatterings of H on H_2 provided are cooling essential to the gravitational collapse of inhomogeneities in the primordial gas and the formation of the first stars. In the galactic interstellar medium, shock heating of the molecular gas

can lead to partial dissociation of H_2, in which case H-H_2 collisions determine the thermal profile and chemical evolution of the postshock gas as it cools to its equilibrium state. In photon-dominated regions of the interstellar medium, which are exposed to sources of ultravoilet radiation, there exists a region of overlap of atomic and molecular hydrogen, where the optical depth in the ultravoilet electronic absorption bands of H_2 becomes sufficient to shield the H_2 deeper in the cloud from the dissociating radiation. The kinetic temperature in this region is controlled by inelastic H-H_2 collisions.

For the formation of star in the cloud, hydrogen is crucial. In the early universe, when the cloud meets the Jean's condition, it starts to collapse. As the collapse continues, the energy created by gravity potential energy should be released by some way. Or the cloud cannot satisfy the condition anymore, the collapse stops. Hydrogen provides an efficient way to release this energy to make the collapse continue without break the Jean's conditions. There are two important conditions for a star to form in the dust. Another is also related with hydrogen, cooling. The cooling is primarily by hydrogen molecule.

Hydrogen also provides an effective way to study the phenomenon of astrophysics. In the shocked region, there is a large emission from H_2. Observed H_2 line ratio could be explained by a phenomena called a bow shock. X-ray illuminated regions such as active galaxies, star burst galaxies also produce hot H_2 emission.

H₃ POTENTIAL SURFACES
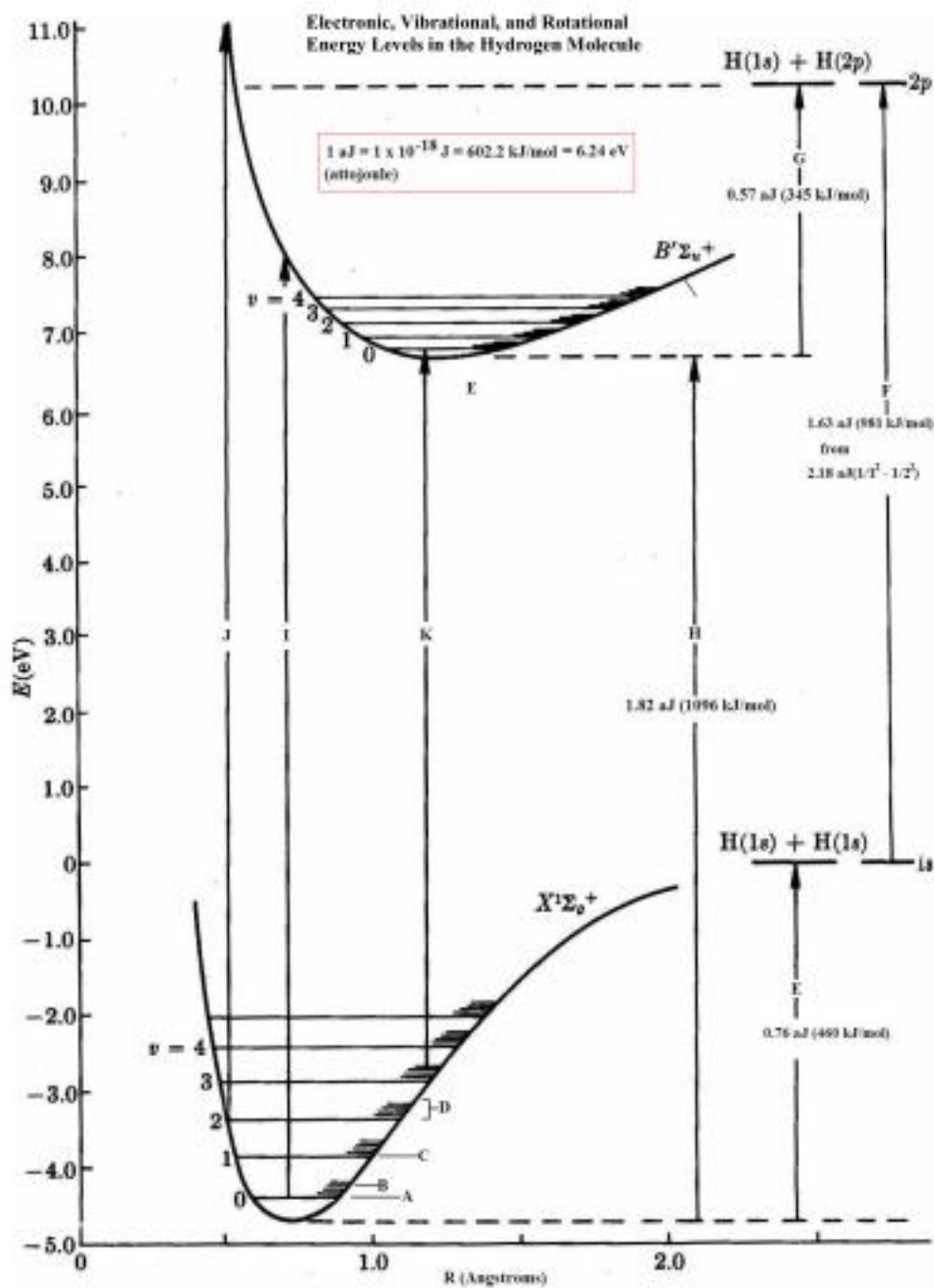
Figure 1   H₂ Potential Surface

Here is the potential surface of H_2. The transitions we study focus on ground potentials. For H_3 potential surface, it is much more complicated.

The H_3 potential surface has developed for a long time. According to the method used to solve H_2 potential surface, we extend to H_3. Assuming the three atoms are at fixed coordinates, and determine a potential energy surface in the three coordinates which are required to describe the relative positions of three atoms. This procedure is the Born-Oppenheimer approximation. London's potential is thought to be earliest work for this area. After it, the most well known potentials are LSTH[6] (Liu-Seigbahn-Truhlar-Horowitz), DMBE[7] (double many-body expansion) and BKMP[8] & BKMP2[9] (Boothroyd-Keogh-Martin-Peterson). The most recent ones are Extensive Quantum Monte Carlo (EQMC)[10] and Mielke. Generally, they fit more theoretical calculation points as the time goes on.

London's potential surface[11] is one of the earliest examples for H_3 potential surface. Though it did not agree well with the experimental data, it built up the basic technique for all the early calculations.

One of the early ab initio calculations of the H_3 potential surface used variational methods to compute the potential for linear symmetric configuration of the three hydrogen atoms[12]. This method improved a lot. Even though, most of the earlier ab initio surface did not agree well with existing experimental results.

The early LSTH potential energy surface was developed by Liu using a potential energy surface for linear H_3. It is reasonable to use a one dimensional Born-Oppenheimer approximation to determine the potential energy surface for the

motion of the three nuclei on a collinear geometry. Then Siegbahn and Liu[13] extended the potential to three dimensions. The later LSTH potential is improved by Truhlar and Horowitz[14], making a least-squares analytical fit to it.

DMBE potential is created by Varandas, Brown, Mead, and Truhlar, using a new analytic fit to more existing points. This fits used 316 points of the potential surface to determine the analytical fit. "It is claimed by Varandas et al. That their potential is superior to the LSTH potential at intermediate and long-range separations of H and H_2." Here the condition is critical to this qualitative assessment.

The BKMP potential extended the LSTH surface based on a more extensive grid of ab initio interaction energies.

BKMP2 potential is more accurate than the DMBE or LSTH potentials, an analytical fit to 8701 points. However, the experimental evidence showed it is less accurate as presented in Banares[15] in regions of the potential energy surface.

EQMC (Extensive Quantum Monte Carlo) potential and Mielke's potential are more recent than the one above.

In the potential Born-Oppenhermer approximation[16], the interactions of the electrons are accounted for by a potential surface. The most accurate available potential surface is by Mielke. The Mielke potential surface should yield more accurate scattering data, particularly near-threshold cross sections and the corresponding low-temperature rate coefficients.

In our calculations, we prefer the Mielke potential, comparing with the previous potentials. In the following part, we are going to talk about Mielke's potential.

Mielke's Potential Surface

The Mielke performed MRCI calculation at 4067 configurations with the standard

aug-cc-pVDZ,aug-cc-pVTZ, and aug-cc-pVQZ basis sets.

Mielke potential fits best with collinear van der Waals.

Consider corrections to the Born-Oppenheimer approximation, that have not been

included yet in H_3 surfaces. Mielke improved the potential by two ways as below:

Basis Set Extrapolation[17][18]:

$$V_{ABC} = \sum V_A^{(1)} + \sum V_{AB}^{(2)} + \sum V_{ABC}^{(3)}$$

Where $V_A^{(1)}$ is the energy of an isolated atom A, and $V_{AB}^{(2)}$ and $V_{ABC}^{(3)}$ are two-

and three-body interaction energies, respectively.

$$E_{CBS}^{3-body} = E_i^{3-body} + \frac{\left(E_i^{3-body} - E_j^{3-body} \right) + \left(E_{CBS}^{2-body} - E_i^{2-body} \right)}{\left(E_i^{2-body} - E_j^{2-body} \right)}$$

Where E_{CBS}^{n-body} denotes the sum of all the n-body energies, i and j denote the two

basis sets used, and it requires i > j.

Fitting: the functional form is taken to be a London potential[19], augmented with a

three-center correction

$$V = V_{London} + V_{3C}$$

Because of the completeness of basis-set, the Mielke potential has the highest

accuracy. Also it has better harrier height, van der vaals well depth, and lowest energy

conical intersection. Compare with earlier analytic H_3 potential surfaces, it displays a

considerably improved representation of the long-range anisotropy which is expected

to be important for the accurate description of low energy scattering processes.

CHAPTER 4

SOLUTION OF H_3 PROBLEM

There are several steps to solve the H_3. First, we need to solve the wave function. Here we use the time-independent wave function. Second, apply the proper potential surface into the wave function. Then we can use the program to calculate the function. From the result of ABC program, we can calculate cross section and compare with previous works. The transitions between different energy levels of H_3 contain collisional transition and radiation transition. In our calculation, we only consider the collisional transition here.

The way to solve H_3 problem developed a lot. We are going to discuss different ways to solve this problem, both advantage and disadvantage.

Classical Trajectory

The classical trajectory use a large number of randomly chosen classical trajectories for a given impact parameter that are computed using the potential energy surface with initial conditions that are consistent with the desired initial condition in order to compute the desired cross sections[20].

Advantage of this method is significantly less computationally intensive, provide a complete set of cross sections and rate coefficients to high energies in a reasonable time frame. But it cannot give good results at low temperature where purely quantum-mechanical effects contribute to the cross sections. The calculation mainly base on the Newton's law. Assume the potential surface first, get the force from it to

calculate the mechanics.

$$F = ma$$

$$F = -\nabla V$$

Quantum Calculations

In the quantum calculation there are two types, one is time-dependent and another is time-independent. Here is our analysis.

Time-dependent Schrödinger equation：

Time-dependent calculations solve the time-dependent Schrödinger equation:

$$H\psi(\text{r,t}) = i\hbar \frac{\partial \psi(\text{r,t})}{\partial t}$$

For each initial state, S-matrix should be calculated. According to the limit ability of the current computer, it is hard to solve the problem in three dimensions for a realistic potential. We are looking forward the more powerful computer developed.

Time-independent Schrödinger equation：

By separation of variables, the time dependence of the equation can be removed, provided the potential has no explicit time dependence.

Consider time-independent Schrödinger equation.

$$-\frac{\hbar^2}{2m}\nabla^2\psi(r) + V(r)\psi(r) = E\psi(r)$$

Assume that the solution has this form[21]:

$$\psi(\boldsymbol{r},t) = \phi(\boldsymbol{r})\chi(t)$$

Substitute it into the time-dependent Schrödinger equation, at the same time assume no explicit time dependence in the potential. We get:

9

$$i\hbar\phi(\boldsymbol{r})\frac{d\chi}{dt} = -\frac{\hbar^2}{2m}\chi(t)\nabla^2\phi(\boldsymbol{r}) + \chi(t)V(\boldsymbol{r})\phi(\boldsymbol{r})$$

Both sides divided by $\phi(\boldsymbol{r})\chi(t)$

$$\frac{i\hbar}{\chi(t)}\frac{d\chi(t)}{dt} = -\frac{\hbar^2}{2m}\frac{1}{\phi(\boldsymbol{r})}\nabla^2\phi(\boldsymbol{r}) + V(\boldsymbol{r})$$

Now the left side is a function of time and the right side is a function of position,

they can only be equal if both sides are equal to constant E.

Then the left side can be integrated:

$$\chi(t) = Ae^{-i\frac{E}{\hbar}t} = Ae^{-i\omega t}$$

The right side yields the time-independent Schrödinger equation:

$$\left[-\frac{\hbar^2}{2m}\nabla^2 + V(\boldsymbol{r}) \right]\phi(\boldsymbol{r}) = E\phi(\boldsymbol{r})$$

If this equation is expressed in the hyperspherical coordinate, the observables that

can be calculated from the resulting helicity-reprensentation S-matrix elements

$S_{n'k',nk}^{J}(E)$ range from fully state-resolved differential

$$\frac{d\sigma_{n'k'\leftarrow nk}}{d\Omega}(\theta, E) = \left| \frac{1}{2ik_n}\sum_{J}(2J+1)d_{k'k}^{J}(\theta)S_{n'k',nk}^{J}(E) \right|^2$$

and integral

$$d\sigma_{n'k'\leftarrow nk}(\theta, E) = \frac{\pi}{k_n^2}\sum_{J}(2J+1)\left| S_{n'k',nk}^{J}(E) \right|^2$$

Reactive scattering cross sections are thought to have considerably more averaged

quantities such as initial state-selected reaction cross sections and thermal rate

constants.

The coupled-channel hyperspherical coordinate method that is used in the ABC

program is based on the Schrödinger equation:

$$\hat{H}\Psi = E\Psi$$

After apply the truncated range of k quantum numbers, the orbital angular

momentum functions $\left|JMjl\right\rangle$ could be obtained from the orthogonal transformation

$$\left|JMjl\right\rangle = \sum_{k=-\min(J,j,k_{max})}^{\min(J,j,k_{max})} \left|JMjk\right\rangle D_{kl}^{Jj}$$

Where D_{kl}^{Jj} is a component of an eigenvector of the matrix representation of the

operator l^2 in the truncated helicity basis. This matrix representation of l^2 is

tri-diagonal, with diagonal elements

$$\left\langle JMjk\left|l^2\right|JMjk\right\rangle = J(J+1)+j(j+1)-2k^2$$

And off-diagonal elements

$$\left\langle JMjk'\left|l^2\right|JMjk\right\rangle = \left[J(J+1)-k'k\right]^{\frac{1}{2}}\left[j(j+1)-k'k\right]^{\frac{1}{2}}\delta_{|k'-k|,1}$$

If the helicity basis were complete, the elements D_{kl}^{Jj} of the eigenvectors of this

matrix would be:

$$D_{kl}^{Jj} = \left(\frac{2l+1}{2J+1}\right)^{\frac{1}{2}} D(jlJ,k0k)$$

Born Oppenheimer Approximation

In basic terms, it allows the wave function of a molecule to be broken into its

electronic and nuclear (vibrational, rotational) components.

$$\Psi_{total} = \psi_{electronic} \times \psi_{nuclear}$$

First step: In the first step of the BO approximation the *electronic* Schrödinger

equation is solved, yielding the wave function $\psi_{\text{electronic}}$ depending on electrons only.

Second step: In the second step of the BO approximation the nuclear kinetic energy T_n (containing partial derivatives with respect to the components of **R**) is reintroduced and the Schrödinger equation for the nuclear motion is solved.

The Hamiltonian for the H_3 can be written as:

$$H = H_N + H_e$$

Where H_N is the nuclear Hamiltonian and H_e is the electronic Hamiltonian.

The total wave function is:

$$H\Psi_{tot} = E\Psi_{tot}$$

Here we skip the steps how to solve the equation, get this equation below:

$$\sum_{m=0}^{N}\left[\frac{\hbar^2}{2\mu}\sum_{k=0}^{N}\left(-i\delta_{nk}\nabla - A_{nk}\right)\bullet\left(-i\delta_{km}\nabla - A_{km}\right) + \delta_{nm}V_n\right]\psi_n = E\psi_n$$

The BO approximation only consider the first term:

$$\psi_{tot} \approx \psi_0\phi_0$$

Leave only the first eigenvalue equation to determine the wave function:

$$\left[-\frac{\hbar^2}{2\mu}\left(\nabla - iA\right)^2 + V\right]\psi = E\psi$$

This results in the term having the identical form of a magnetic vector potential.

In analogy to the Aharonov-Bohm effect, the processes that encircle the conical intersection would cause the wave function to change sign. So this will affect the H_3 system. We need to properly antisymmetrize the interference of reactive and non-reactive parts of wave function when interchange the three H atoms. This is the source of the change of sign in the interference terms to calculate the integral cross

sections. According to Archer's study of geometric phase effects, exact cancellation of

potential geometric phase effects will not affect the H_3 system integral cross sections.

Identical Particles (three identical particles)

In our ABC program, we use a couple-channel hyperspherical coordinate.
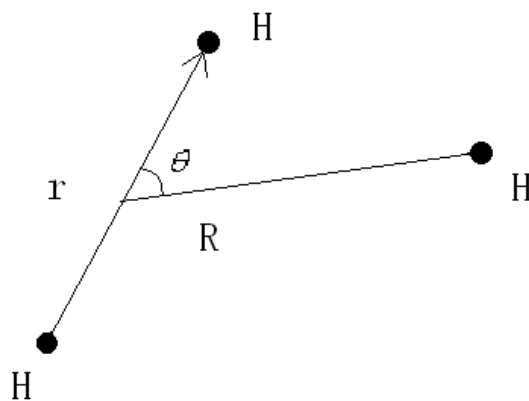
Figure 2   Postions of Three Hydrogen Atoms

In the ABC program, first we treat the three Hydrogen atoms as distinguishable

particles. Assume that the three atoms are at fixed coordinates, and compute this for a

number of inter-nuclear spacings. From this we get an effective potential energy

surface. This procedure is called the Born-Oppenheimer. To get correct results for H_3

system, one must post antisymmetrize the results. The H_3 potential has a conical

intersection where geometric phase effects may manifest. It is not clear that how to

take account in the geometric phase and other effects. To some extent it is potential

dependent, the BKMP2 potential implies there are no geometric phase effects to

account for, while some other potentials imply that there are. Fortunately, for some

reasons that is not clear yet, integral cross sections and rate coefficients do not seem to change in either case.

Cross Section

In nuclear and particle physics, the concept of a cross section is used to express the likelihood of interaction between particles. When particles in a beam are thrown against a foil made of a certain substance, the cross section σ is a hypothetical area measure around the target particles of the substance (usually its atoms) that represents a surface. If a particle of the beam crosses this surface, there will be some kind of interaction.

The term is derived from the purely classical picture of (a large number of) point-like projectiles directed to an area that includes a solid target. Assuming that an interaction will occur (with 100% probability) if the projectile hits the solid, and not at all (0% probability) if it misses, the total interaction probability for the single projectile will be the ratio of the area of the section of the solid (the *cross section*, represented by σ) to the total targeted area.

Classical Mechanics：

In classical mechanics, consider the collision of two particles initially in the internal states described by an index i[22]. To simplify notation, it is convenient to use a single index to specify the states of both particles. The angle between the initial and final relative velocities **v** and **v**' is given by spherical polar coordinates Θ and Φ,

where Θ is the deflection angle in the center of mass frame. We start with a well-defined beam of particles with a flux I_i (number of particles per unit area per unit time). After the collision, the flux I_j (numbers of particles per unit solid angle per unit time) is a function of deflection angle Θ and is different for each possible set of final internal states j. We define the differential cross-section as

$$\frac{d\sigma_{ij}}{d\omega} = \frac{I_j}{I_i}$$

Where ω is an element of solid angle at deflection angle Θ. the corresponding integral cross-section σ_{ij} is integrated over all possible final direction. Note that this quantity has units of area. Furthermore, it depends only on the geometry of the scattering center, and not on the incident flux or distance of the detector from the scattering center. The geometric interpretation is as follows: consider particles that scatter through a solid angle $d\Omega$ and ask what values of impact parameter produced them. These impact parameters form a differential area, $d\sigma$ in space. The differential cross section is simply

$$\frac{d\sigma}{d\Omega}$$

So it contains information about the total probability of the transition i→j,

$$\sigma_{ij} = \int_0^{2\pi} \int_0^{\pi} \left(\frac{d\sigma_{ij}}{d\omega} \right) \sin\Theta \, d\Theta \, d\Phi$$

Quantum Mechanics:

In quantum mechanics, the differential cross section is defined as follows: the wave function of the incident particle is a plane-wave with amplitude 1, that is e^{ikz}. In general the scattered wave is of the form

$$f(\theta,\phi)\frac{e^{ikr}}{r}$$

Then we have

$$\frac{d\sigma}{d\Omega}=|f|^2$$

This has the simple interpretation of the probability of finding a scattered particle within a given solid angle.

The integral cross section is the integral of the differential cross section on the whole sphere of observation (4π steradian):

$$\sigma=\int d\Omega\frac{d\sigma}{d\Omega}$$

A cross section is therefore a measure of the effective surface area seen by the impinging particles, and as such is expressed in units of area. Usual units are the cm^2, the barn (1 b = 10^{-28} m^2) and the corresponding submultiples: the millibarn (1 mb = 10^{-3} b), the microbarn (1 μb = 10^{-6} b), the nanobarn (1 nb = 10^{-9} b), the picobarn (1 pb = 10^{-12} b), and the shed (1 shed = 10^{-24} b). The cross section of two particles (i.e. observed when the two particles are colliding with each other) is a measure of the interaction event between the two particles. The cross section is proportional to the

probability that an interaction will occur; for example in a simple scattering

experiment the number of particles scattered per unit of time (current of scattered

particles I_r) depends only on the number of incident particles per unit of time (current

of incident particles I_i), the characteristics of target (for example the number of

particles per unit of surface N), and the type of interaction.

$$I_r = I_i N \sigma$$

$$\sigma = \frac{I_r}{I_i} \frac{1}{N} = \text{probability of interaction} \times \frac{1}{N}$$

S-Matrix

The S-matrix operator is an operator connecting states in the infinite past with

states in the infinite future. If at some infinite time in the past the wave function had

the form:

$$\Psi(-\infty) = \lim_{t \to -\infty} \Psi(t)$$

For a definite energy and angular momentum, after the interaction takes place the

system is in the state

$$\Psi(\infty) = \lim_{t \to \infty} \Psi(t)$$

then

$$\Psi(\infty) = S\psi(-\infty)$$

In the scattering， the S-matrix is the matrix elements of the S operator that

connects the initial and final states. The S operator is a unitary operator to keep the

energy conserved (the total probability for something to happen to be unity). Thus the

S-matrix value squared is the probability that a given input wave function will result

in a given output wave function, or in the time independent case the S-matrix value

squared represents the fractional contribution that a given outgoing wave function

basis function contributes to the total outgoing wave function.

For a particular basis set $\left| \varphi_i \right\rangle$, the outgoing asymptotic wave function can be

determined using the S operator

$$\left| \psi_{out} \right\rangle = S \left| \varphi_i \right\rangle$$

The amplitude to observe a given outgoing basis state $\left| \varphi_j \right\rangle$, is got by

$$\left\langle \varphi_j \middle| \psi_{out} \right\rangle = \left\langle \varphi_j \middle| S \middle| \varphi_i \right\rangle = S_{j \leftarrow i}$$

The probability of a given transition between two of the basis set states in a

collision is

$$P = \left| \left\langle \varphi_j \middle| S \middle| \varphi_i \right\rangle \right|^2 = \left| S_{j \leftarrow i} \right|^2$$

Relation to the S Matrix：

If the reduced masses and momenta of the colliding system are m_i, $\overrightarrow{p_i}$ and m_f,

$\overrightarrow{p_f}$ before and after the collision respectively, the differential cross section is given

by

$$\frac{d\sigma}{d\Omega} = (2\pi)^4 m_i m_f \frac{p_f}{p_i} \left| T_{fi} \right|^2$$

Where the on-shell T matrix is defined by

18

$$S_{fi} = \delta_{fi} - 2\pi i \delta(E_f - E_i)\delta(\vec{p_i} - \vec{p_f})T_{fi}$$

In terms of the S matrix, the δ function is the distribution called the Dirac delta

function. The computation of the S-matrix is the main aim of the scattering theory.

CHAPTER 5

ABC PROGRAM

ABC program is a general purpose atom-diatom time-independent reactive

scattering program that can be used to compute state-to-state scattering matrix values,

including both reactive and non-reactive channels. A lot of the previous work only

considers the reactive part of the calculation, without handling the symmetry

correctly.

The program uses a coupled-channel hyperspherical coordinate method to solve

the Schrödinger equation for the motion of the three nuclei (A, B and C) on a single

Born-Oppenheimer potential energy surface. The coupled-channel method used

involves a simultaneous expansion of the wave function in the Delves hyperspherical

coordinates of the three chemical arrangements (A+BC, B+CA,C+AB). The quantum

reactive scattering boundary conditions are applied exactly, without the use of an

imaginary absorbing potential, and the coupling between orbital and rotational

angular momentum is also implemented correctly for each value of the total angular

momentum quantum number.

In each separate run of the ABC program, the reactive scattering Schrödinger

equation is solved for specified values of the total angular momentum quantum

number J and the triatomic parity eigenvalue P, and also in the case of A+B$_2$ reactions

for a specified value of the diatomic parity eigenvalue p(where $p=+1$ for even and -1

for odd rotational states of the B$_2$ molecule). Each (J,P,$p)$ tiple therefore requires a

different calculation, as indicated for some example reactions in Table 1.

Table 1 Required Values of *J*, *P* And *p* For Various Reactions

reaction	*J*	*P*	*p*
A+B$_2$(j=0)	0, 1, 2, ...	$(-1)^J$	+1
A+B$_2$(j>0)	0	+1	$(-1)^J$
	1, 2, 3, ...	± 1	$(-1)^J$
A+BC(j=0)	0, 1, 2, ...	$(-1)^J$	n/a
A+BC(j>0)	0	+1	n/a
	1, 2, 3, ...	± 1	n/a

The resulting output files contain parity-adapted scattering matrix elements of the

form $S^{J,P}_{\alpha'v'j'k',\alpha vjk}(E)$, where α and α' are arrangement labels, v and v' are diatomic

vibrational quantum numbers, j and j' are diatomic rotational quantum numbers, k and

k' are helicity (intermolecular axis angular momentum projection) quantum numbers.

The primed quantities refer to the products of the reaction and unprimed quantities to

the reactants, with $\alpha = 1$ for the A+BC, $\alpha' = 2$ for the B+CA and $\alpha' = 3$ for the

C+AB. The argument E of the scattering matrix is the total (collision plus internal)

energy measured from the bottom of the asymtotic reactant valley.

Once these scattering matrix elements have been calculated for sufficiently many

values of *J* and for energies, they can be used to compute any observable property of

the reaction. The first stage in this process is to convert the parity-adapted S-matrix

elements $S^{J,P}_{n'k',nk}(E)$ into standard helicity-representation S-matrix elements

$S^{J}_{n'k',nk}(E)$ using the formulas:

$$S^{J}_{n'k',nk} = S^{J}_{n'-k',n-k}(E) = \frac{\sqrt{(1+\delta_{k'0})(1+\delta_{k0})}}{2}[S^{J,+1}_{n'k',nk} + S^{J,-1}_{n'k',nk}]$$

(1)

21

And

$$S^J_{n'-k',nk} = S^J_{n'k',n-k}(E) = (-1)^J \frac{\sqrt{(1+\delta_{k'0})(1+\delta_{k0})}}{2}[S^{J,+1}_{n'k',nk} - S^{J,-1}_{n'k',nk}]$$
(2)

Where n and n' are composite indices for αvj and $\alpha'v'j'$ and the quantum

numbers k and k' are restricted such that $0 \le k \le \min(J,j)$ and

$0 \le k' \le \min(J,j)$.(the quantum numbers k=0 and k'=0 only occur in the parity block

with $P = (-1)^J$, but equation (1) and (2) have been written with this in mind: simply

set $S^{J,P}_{n'k',nk} = 0$ whenever $P = (-1)^{J+1}$ and k and/or $k' = 0$.)

The observables that can be calculated from the resulting helicity-representation

S-matrix elements $S^J_{n'k',nk}(E)$ range from fully state-resolved differential:

$$\frac{d\sigma_{n'k'\leftarrow nk}}{d\Omega}(\theta,E) = \left|\frac{1}{2ik_n}\sum_J (2J+1)d^J_{k'k}(\theta)S^J_{n'k',nk}(E)\right|^2$$

And integral:

$$\sigma_{n'k'\leftarrow nk}(\theta,E) = \frac{\pi}{k_n^2}\sum_J (2J+1)\left|S^J_{n'k',nk}(E)\right|^2$$

In which,

$$k_n = \frac{2uE_{kin}}{\hbar^2}$$

CHAPTER 6

SUMMARY AND CONCLUSION

The convergence test was checked in Archer's work and the same parameters were used for this calculation as Archer used (Archer 2006). A program written in Java was used to calculate the final cross section (Gobeli 2012 private communication).

Since there is few experiment data to compare, we mainly compare our results with the previous work. Because the ABC code and Mielke's potential are the best choice to deal with this problem (the author of BKMP also recommend Mielke's potential), our result can be thought as the most accurate data now. This can be seen from the comparison with previous work.

From the data we calculate, we make the graphs below. In figure 3, at the low kinetic energy, the curve grows rapidly (for v, j (0,0)→(0,2), there is some fluctuation); at around 0.5 ev, the curve turn into flat. That means when it is at the low temperature, the change of temperature affects the cross section a lot. A small change of temperature can result in big fluctuation of cross section. Once the temperature is high enough (still in a certain range), the cross section reaches its top, and is not that sensitive to the temperature any more, almost becoming stable. This is related with the certain transitions energies between different energy levels. Also the lowest kinetic energy to arouse the transition varies with different transitions.

Figure 3　　Cross Section vs Kinetic Energy For v,j: (0,0)→(0,2), (0,1)→(0,3), by ABC Using Mielke's Potential

Cross Section vs Kinetic Energy
(ABC using Mielke PES)
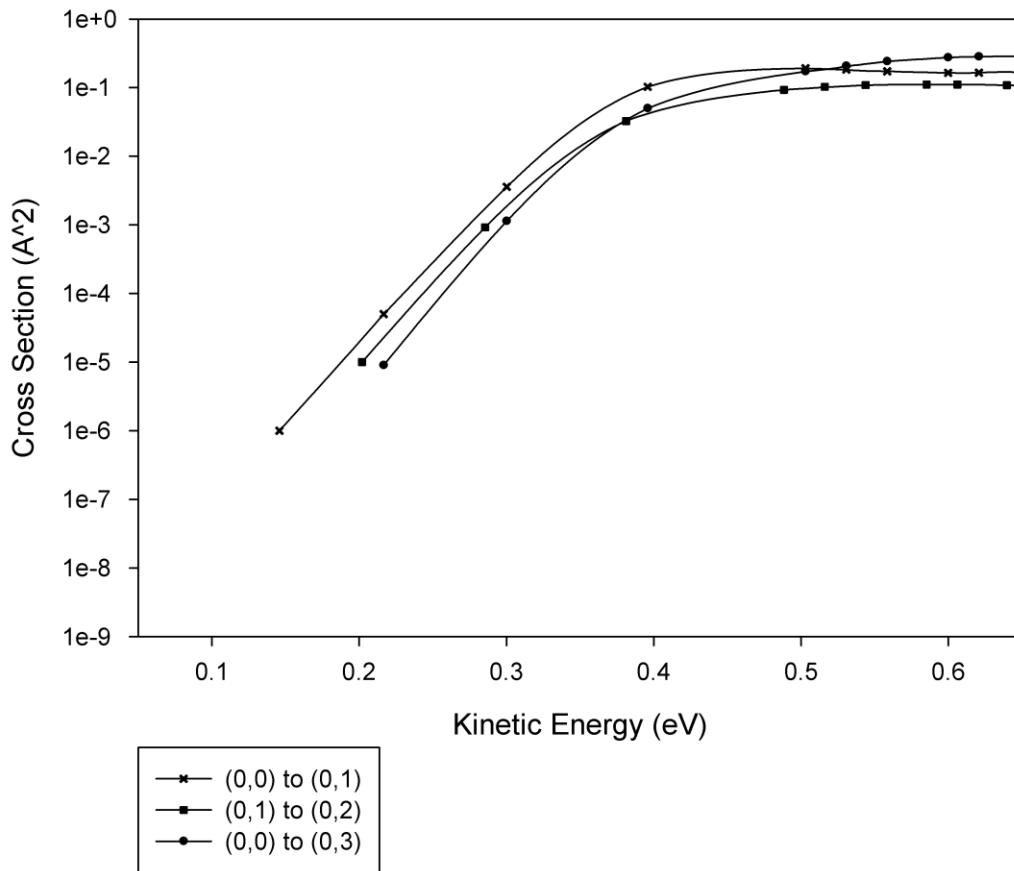
Figure 4   Cross Section vs Kinetic Energy, For v,j: $(0,0) \rightarrow (0,1)$, $(0,1) \rightarrow (0,2)$,

$(0,0) \rightarrow (0,3)$ by ABC Using Mielke's Potential

Here, in the figure 4, we have the cross sections for the transitions for v, j:

$(0,0) \rightarrow (0,1)$, $(0,1) \rightarrow (0,2)$, $(0,0) \rightarrow (0,3)$. For these three transitions, the curves are

similar. We also notice that the difference between different transitions is related with

j is even or odd. There is almost one magnitude between each. I make a figure 5 about

how $|S|^2$ value changes with J value, when J's value follows different curves when it

is even or odd.
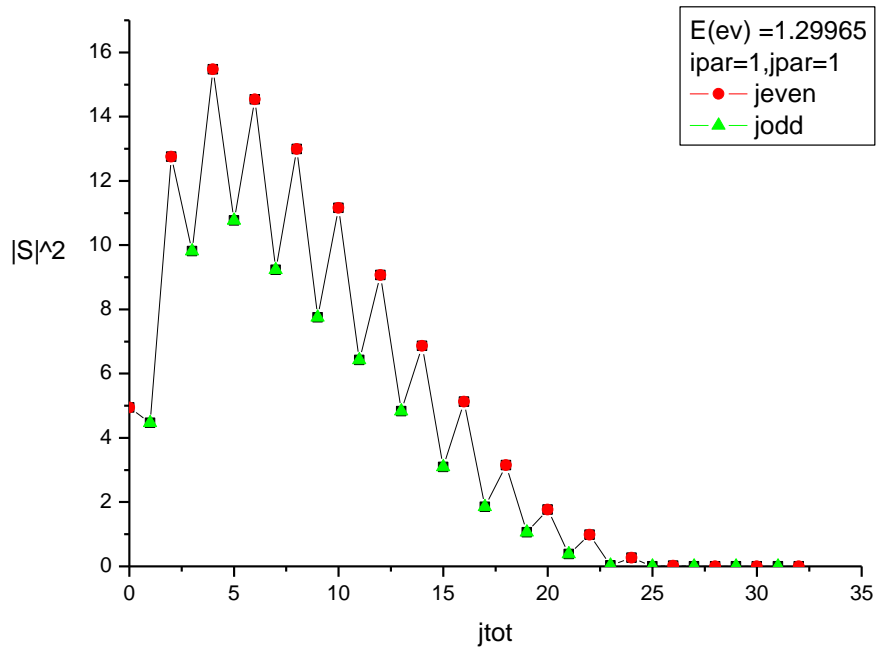
Figure 5 |S|^2 Value vs Total Angular Momentum Quantum Number J, At Total

Energy E=1.29965 ev
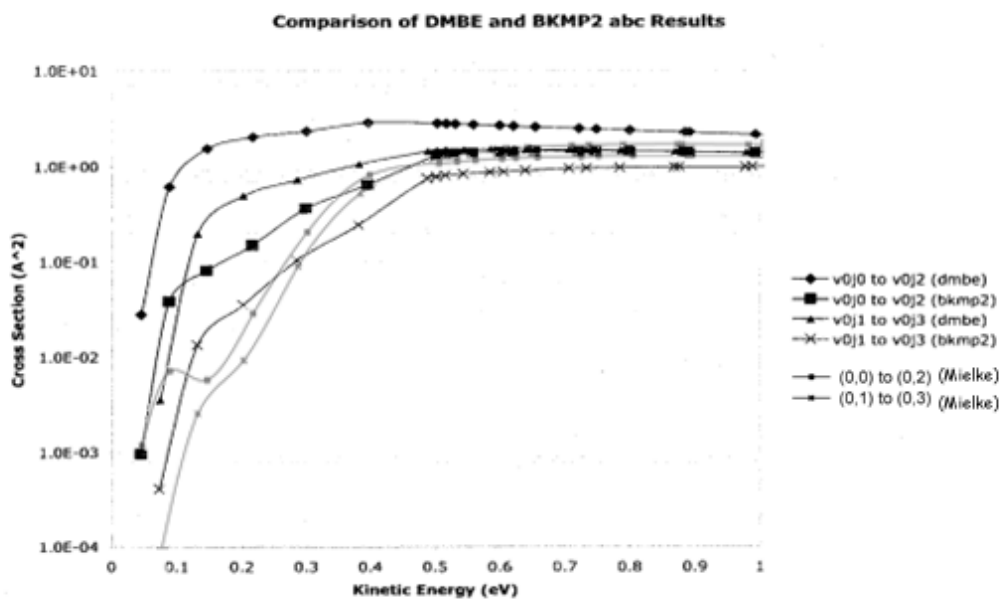
Figure 6   Cross Section Vs Kinetic Energy, Comparison Of DMBE, BKMP2,
Mielke Using   ABC Code

In the figure 6, we compare our results with DMBE and BKMP2 potentials, all calculated by ABC code. Because there is no data of the work done by Archer, this graph is produced by combining two graphs in the same scale. In high kinetic energy (higher than 0.5 ev), three different potential's curves are consistent with each other. Significant differences exist at the low kinetic energies, both on the quantity level and curve's shape. The cross sections from Mielke are closer to BKMP2 (which is thought more accurate than potentials before it) than DMBE, but still lower than BKMP2 in some area obviously. While at the high energy, the curves agree better. How to describe the potential is critical to study the collision of atoms at low temperature. We also make a compare with another calculation result using Mielke's potential by MOLCOL code[23]. See figure 7, black solid lines, it calculated the cross section for J= 2→0 transition, which is related with J=0→2 done in our calculation. At the low temperature, for some part of the line, the value drops and then returns to rise, having a similar shape with ours.

We compare with the work done in Archer. The dark line is our data in this paper. The agreement is good both at low energy and high energy. Again our data seem to agree with BKMP2 better than DMBE. Both of BKMP2 and Mielke treat H_3 system as three indistinguishable particles, and properly antisymmetrize the results. It is reasonable for these two potentials fit with each more than others.

Cross Section vs Kinetic Energy
ABC using DMBE, BKMP2, Mielke
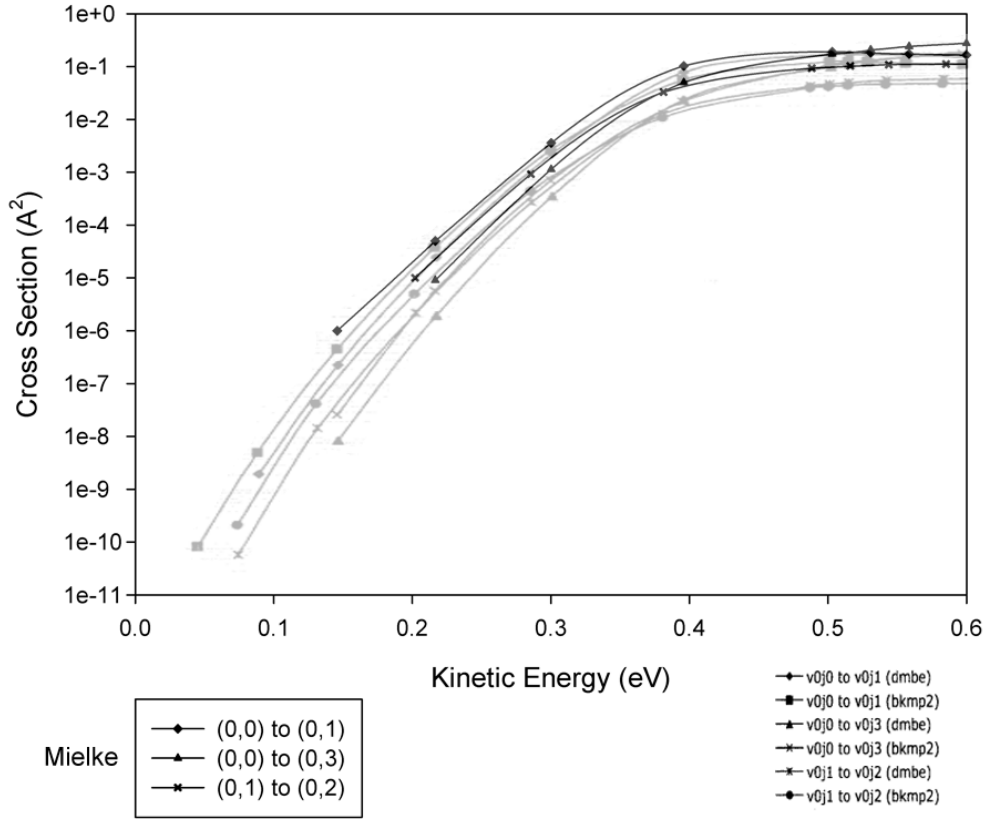
Figure 7   Cross Section vs Kinetic Energy, Comparison of DMBE, BKMP2, Mielke

Using ABC Code

For future's work, we will calculate additional energies and states at high

temperature to get a full view of cross section curve. For higher energies, the time to

calculate them will much longer. According to the previous work, the curve will start

to fall after reach the peak. At the low energies, more points should be calculated to

help to study the quantum behaviors there. Because of the small magnitude of cross

sections at low energies, improving the ABC program to a more accurate level will

help to get better data. So we can build a large database for H_3 case. We can try to

calculate the rate coefficient for the cooling process. Maybe we will also extend to

calculate a cooling curve from these cross sections.

REFERENCES

1. D. Skouteris, J. Castillo, D. Manopoulos, "ABC: Aquantum Reactive Scattering Program", Comp. Phys. Comm., 133, 128, April 2000

2. S. Mielke, B. Garrett, K.Peterson, "A Heirarchical Family of Global Analytic Born-Oppenheimer Potential Energy Surfaces for the H-H2 Reaction Ranging in Quality From Double-zeta to the Complete Basis Set Limit.", J. Chem. Phys., Vol 166, No. 10, 4142, March 2002

3. David Michael Archer, "Quantum Mechanical H-H_2 Collisional Cross Section Calculation for Astrophysics", 2006

4. Boothroyd, A.I., Keogh, W. J., Martin, P. G., & Peterson, M. , J. Chem Phys. 104, 7139 (1996)

5. Bethe and Salpeter, "Quantum mechanics of one and two electro", http://books.google.com/books/about/Quantum_mechanics_of_one_and_two_electro.html?id=1ZUuAAAAIAAJ

6. B. Liu, "Ab Initio Potential Energy Surface for Linear H3", J. Chem. Phys., Vol 58, No. 5, March 1973

7. S. Lepp, M. Shull, " Molecules in the Early Universe", Ap. J. 280: 465-469, May 1984

8. A. I. Boothroyd, W. J. Keogh, P. G. Martin, and M.R. Peterson, J. Chem. Phys. 95, 4343 (1991)

9. L. Banares, M. D'Mello, "Quantum Mechanical Rate Constants for the D+H2 -> HD+H Reaction on the BKMP2 Potential Energy Surface", Chem. Phys. Letters 277 (1977) 465-472

10. Y. Wu, A. Kupperman, J. Anderson, " A Very High Accuracy Potential Energy Surface for H3", Phys Chem. Chem Phys, 1999, 1, 929

11. F. London, Zeits, f. Physick, 46, 455, 1928

12. J. Hirschfelder, H. Eyring, and N. Rosen, " I. Calculation of Energy of H3 Molecule", J. Chem. Phys, 4, 121, February 1936

13. P. Seigbahn, B. Liu, "An Accurate Three-Dimensional Potential Energy Surface For H3", J. Chem. Phys., 68, 2457, March 1978

14. D. Truhlar, C. Horowitz, "Functional Representation of Liu And Siegbahn's Accurate Ab Initio Potential Energy Calculations for H+H2", J. Chem, Phys, 68, 2466, March 1978

15. L. Banares, M.D'Mello, "Quantum Mechanical Rate Constants for the D+H2 -> HD+H Reaction on the BKMP2 Potential Energy Surface", Chem. Phys. Letters 277 (1977) 465-472

16. M. Born, J. Oppenheimer, Ann. Physik, 84 (1927) 457

17. A. J. C. Varandas and J. N. Murrell, Faraday Discuss. Chem. Soc. 62, 92 (1977)

18. J. N. Murrell, S. Carter, S. C. Farantos, P. Huxley, and A. J. C. Varandas, Molecular Potential Energy Functions (Wiley, London, 1984)

19. F. London, Z. Elektrochem. Angew. Phys. Chem. 35, 552 (1929)

20. David Michael Archer, "Quantum Mechanical H-H_2 Collisional Cross Section Calculation for Astrophysics", 2006

21. C. Cohen-Tannoudji, B. DiU, F. Laloe, Quantum Mechanics Volume One, (Wiley Interscience, 1977)

22. Roman V. Krems, William C. Stwalley, Bretislav Friedrich, "Cold Molecules"

23. S A Wrathmall and D R Flower, 2006 J. Phys. B: At. Mol. Opt. Phys. 39 L249

VITA

Graduate College
University of Nevada, Las Vegas

Qianxia Zou

Degrees:
    Bachelor of Science, Physics, 2009
    Southeast University, China

Thesis Title: New Cross Sections for H on H_2 Collisional Transitions

Thesis Examination Committee:
    Chairperson, Dr. Stephen Lepp, Ph. D.
    Committee Member, Dr. Tao Pang, Ph. D.
    Committee Member, Dr. Bing Zhang, Ph. D.
    Graduate Faculty Representative, Dr. Balakrishnan Naduvalath, Ph. D.